Statistical mechanics of canonical-dissipative systems and applications to swarm dynamics

Frank Schweitzer*
Real World Computing Partnership—Theoretical Foundation, GMD Laboratory, Schloss Birlinghoven, 53754 Sankt Augustin, Germany

Werner Ebeling†
Institute of Physics, Humboldt University, Invalidenstraße 110, 10115 Berlin, Germany

Benno Tilch‡
II. Institute of Theoretical Physics, University of Stuttgart, Pfaffenwaldring 57/III, D-70550 Stuttgart, Germany
(Received 16 March 2001; published 27 July 2001)

We develop the theory of canonical-dissipative systems, based on the assumption that both the conservative and the dissipative elements of the dynamics are determined by invariants of motion. In this case, known solutions for conservative systems can be used for an extension of the dynamics, which also includes elements such as the takeup/dissipation of energy. This way, a rather complex dynamics can be mapped to an analytically tractable model, while still covering important features of nonequilibrium systems. In our paper, this approach is used to derive a rather general swarm model that considers (a) the energetic conditions of swarming, i.e., for active motion, and (b) interactions between the particles based on global couplings. We derive analytical expressions for the nonequilibrium velocity distribution and the mean squared displacement of the swarm. Further, we investigate the influence of different global couplings on the overall behavior of the swarm by means of particle-based computer simulations and compare them with the analytical estimations.

DOI: 10.1103/PhysRevE.64.021110 PACS number(s): 05.40.−a, 05.45.−a

I. INTRODUCTION

The collective motion of biological entities, like schools of fish, flocks of birds, herds of hoof animals, or swarms of insects, has recently also attracted the interest of physicists. Here, the question of how a long-range order between the moving entities can be established is of particular interest. Consequently, some of the more biologically centered questions of swarming behavior, namely, questions about the reasons for swarming and the group size dependence, have been dropped so far in physical swarm models. The main focus was rather on the emergence of coherent motion in a ''swarm'' of locally or globally coupled particles.

For the coupling different assumptions have been proposed (cf. also Sec. IV), such as the coupling of the particles' individual orientations (i.e., directions of motion) to the mean orientation of the swarm [1,2], or the coupling of the particle's individual position to the mean position (center of mass) of the swarm [3]. On the other hand, other local couplings have also been considered, such as the coupling of the particle's individual velocity to a local average velocity [2,4–6]. A different class of models further assumes a local coupling of the particles via a self-consistent field that has been generated by them [7,8]. This models the case of chemical communication between the particles widely found in biology. For example, the streaming behavior of myxobacteria [9–11], the directed motion of ants [12–14] and the coherent movement of cells [15] have been described and modeled by means of this kind of local coupling.

But long-range or short-range coupling of the particles is only one of the prerequisites that account for swarming. Another one is the *active motion* of the particles. Of course, particles can also move passively, driven by thermal noise, by convection, currents or by external fields. This kind of driving force, however, does not allow the particle to change its direction of motion, velocity, etc., *itself*. Recent models of *self-driven* particles that are used to simulate swarming behavior [5,16,17] usually just postulate that the entities move with a certain nonzero velocity, without considering the *energetic* implications of active motion. In order to do so, we need to consider that the many-particle system is basically an *open* system that is driven into nonequilibrium.

To this end, our approach to swarming is based on the theory of *canonical-dissipative systems*. This theory—which is not so well known even among experts—results from an extension of the statistical physics of Hamiltonian systems to a special type of dissipative system, the so-called canonical-dissipative system [18–24]. The term *dissipative* means here that the system is nonconservative and the term *canonical* means that the dissipative as well as the conservative parts of the dynamics are both determined by a Hamilton function H (or a larger set of invariants of motion; see Sec. II for details).

This special assumption allows in many cases exact solutions for the distribution functions of many-particle systems, even in far-from-equilibrium situations. This was known already to pioneers such as Poincaré, Andronov, and Bautin, who gave exact solutions for a special class of nonlinear oscillators [25]. In recent work [26] the properties of canonical-dissipative systems were used to find exact solu-

*Electronic address: schweitzer@gmd.de
http://ais.gmd.de/~frank/
†Electronic address: ebeling@physik.hu-berlin.de
http://summa.physik.hu-berlin.de/tsd/
‡Electronic address: benno@theo2.physik.uni-stuttgart.de
http://www.theo2.physik.uni-stuttgart.de/

tions for *dissipative systems* in Toda lattices that are pumped with free energy from external sources. The starting point was the well-known Toda theory of soliton solutions in one-dimensional lattices with a special nonlinear potential (exponential for compression and linear for expansion) of the springs [27,28], which was then extended to a nonconservative system [18,22,23]. In another work [29] an application to systems of Fermi and Bose particles was given.

In this paper, we will apply the theory of canonical-dissipative systems to the dynamics of swarms. We start with an outline of the general theory in Sec. II, describing first the deterministic and then the stochastic approach. As a first step towards the dynamics of swarms, in Sec. III we investigate the *energetic conditions* of swarming, i.e., we discuss the conditions for active motion and their impact on the distribution function and the mean squared displacement of the particles. In Sec. IV we introduce *global interactions* between the particles that may account for swarming, i.e., for the maintenance of *coherent* motion of the ensemble. The global interactions are chosen with respect to the general theory of canonical-dissipative systems. By means of computer simulations we show how different kinds of couplings affect the overall behavior of the swarm. In Sec. V we conclude with some ideas on how to generalize the approach presented in this paper.

II. GENERAL THEORY OF CANONICAL-DISSIPATIVE SYSTEMS

A. Dynamics of canonical-dissipative systems

Let us consider a mechanical many-particle system with f degrees of freedom $i=1,\ldots,f$ and with the Hamiltonian $H(q_1\cdots q_f,p_1\cdots p_f)$. The corresponding equations of motion are

$$\frac{dq_i}{dt}=\frac{\partial H}{\partial p_i},\quad \frac{dq_i}{dt}=-\frac{\partial H}{\partial q_i}. \tag{1}$$

Each solution of the system of equations (1),

$$p_i=p_i(t),\quad q_i=q_i(t), \tag{2}$$

defines a trajectory on the plane $H=E=\text{const}$. This trajectory is determined by the initial conditions, and also the energy $E=H(t=0)$ is fixed due to the initial conditions. We now construct a *canonical-dissipative system* with the same Hamiltonian, where $g(H)$ denotes the *dissipation function*:

$$\frac{dp_i}{dt}=-\frac{\partial H}{\partial q_i}-g(H)\frac{\partial H}{\partial p_i}. \tag{3}$$

In order to elucidate this kind of canonical-dissipative dynamics, we will consider different examples for the dissipation function in the following. In general, we will only assume that $g(H)$ is a nondecreasing function of the Hamiltonian. The canonical-dissipative system, Eq. (3) [18,22,23], does not conserve the energy because of the following relation:

$$\frac{dH}{dt}=-g(H)\sum_i\left(\frac{\partial H}{\partial p_i}\right)^2. \tag{4}$$

Whether the total energy increases or decreases consequently depends on the form of the dissipation function $g(H)$. In the simplest case, we may consider a constant friction:

$$g(H)=\gamma_0>0. \tag{5}$$

As long as $g(H)$ is always positive, the energy always decays.

In a more interesting case the dissipative function $g(H)$ has a root for a given energy E_1: $g(E_1)=0$. Let us further assume that at least in certain neighborhoods of E_1 the function $g(H)$ is increasing. With these assumptions the states with $H<E_1$ are pumped with energy due to the negative dissipation, while energy is extracted from the states with $H>E_1$. That means that any given initial state with $H(t=0)<E_1$ will increase its energy until it reaches the shell $H(t)=E_1$, while any given initial state with $H(t=0)>E_1$ will decrease its energy until the shell $H(t)=E_1$ is reached, too. Therefore, the solution of Eq. (4) converges to the energy surface $H=E_1$. On this surface the solution of Eq. (3) agrees with one of the possible solutions of the original Hamiltonian Eq. (1) for $H=E_1$.

The simplest ansatz for $g(H)$ with a root $g(H)=0$ is a *linear* dissipation function:

$$g(H)=C(H-E_1). \tag{6}$$

With respect to Eq. (4) and the discussion above, it is obvious for this case that the process comes to rest when the shell $H(t)=E_1$ is reached. The relaxation time is proportional to the constant C^{-1}.

We note that the linear dissipation function Eq. (6) has found applications in Toda chains [26]. Here, the fact that on the shell $H=E_1$ the trajectory should obey the original *conservative* canonical dynamics has been used to derive exact solutions for canonical-*dissipative* Toda systems.

A rather general *nonlinear* and nondecreasing dissipation function, which has been proposed in [29], reads

$$g(H)=\gamma_0-\gamma_1\frac{(1+A)}{1+A\exp(\beta H)}. \tag{7}$$

Here $\gamma_0>0$ represents the normal positive friction and $\gamma_1>0$ represents a kind of negative friction. A is a dimensionless constant and β is a parameter denoting a reciprocal temperature. For $\gamma_1\leqslant\gamma_0$ the friction is always positive, i.e., energy is extracted. For the opposite case, $\gamma_1>\gamma_0$, we have negative friction and the system is pumped with energy at least in some parts of the phase space. This allows one to drive the system into situations far from equilibrium. Therefore, in the following we may assume $\gamma_1>\gamma_0>0$.

In the limit $\beta\to 0$ and $A\to 0$ the dissipative function Eq. (7) reduces to the linear case, Eq. (6), discussed above. On the other hand, for small values of β and finite A we get

$$g(H)=\gamma_0-\gamma_1\frac{(1+A)}{1+A+A\beta H}, \tag{8}$$

which yields $g(H)\to(\gamma_0-\gamma_1)<0$ for $H\to 0$, and $g(H)\to\gamma_0$ if $H\to\infty$. This way, the existence of a root $g(E_1)=0$ is always guaranteed.

Before investigating a special case for $g(H)$ in Sec. III, let us introduce a generalization of the formalism. Instead of a driving function $g(H)$ that depends only on the Hamiltonian, we may include the dependence on a larger set of invariants of motion, $I_0,I_1,I_2,\ldots,I_s$, for example: (a) Hamiltonian function of the many-particle system, $I_0=H$; (b) total momentum of the many-particle system, $I_1=P$; (c) total angular momentum of the many-particle system, $I_2=L$. The dependence on these larger sets of invariants may be considered by defining a *dissipative potential* $G(I_0,I_1,I_2,\ldots)$. The canonical-dissipation equation of motion, Eq. (3), is then generalized towards

$$\frac{dp_i}{dt}=-\frac{\partial H}{\partial q_i}-\frac{\partial G(I_0,I_1,I_2,\ldots)}{\partial p_i}. \tag{9}$$

Using this generalized canonical-dissipative formalism, by an appropriate choice of the dissipative potential G the system may be driven to particular subspaces of the energy surface, e.g., the total momentum or the angular momentum may be prescribed. Different examples of this will be also discussed in Sec. IV.

B. Stochastic theory of canonical-dissipative systems

We will now investigate an approach to the stationary probabilities that is based on Langevin and Fokker-Planck equations. The Langevin equations are obtained by adding a white noise term $\xi_i(t)$ to the deterministic Eq. (3),

$$\frac{dp_i}{dt}=-\frac{\partial H}{\partial q_i}-g(H)\frac{\partial H}{\partial p_i}+[2D(H)]^{1/2}\xi_i(t). \tag{10}$$

The essential assumption is that both the strength of the noise, expressed in terms of $D(H)$, and the dissipation, expressed in terms of the friction function $g(H)$, depend only on the Hamiltonian H.

With respect to Eq. (10), the corresponding Fokker-Planck equation for the probability distribution $\rho(q_1\cdots q_f,p_1\cdots p_f)$ of the many-particle system reads

$$\frac{\partial\rho}{\partial t}+\sum p_i\frac{\partial\rho}{\partial q_i}-\sum\frac{\partial H}{\partial p_i}\frac{\partial\rho}{\partial p_i}=\sum\frac{\partial}{\partial p_i}\left[g(H)\rho+D(H)\frac{\partial\rho}{\partial p_i}\right]. \tag{11}$$

An exact stationary solution of Eq. (11) reads

$$\rho^0(q_1\cdots q_f,p_1\cdots p_f)=Q^{-1}\exp\left(\int_0^H dH'\frac{g(H')}{D(H')}\right). \tag{12}$$

The derivative of ρ^0 vanishes if $g(H)=0$, which means that the probability distribution is maximal at the surface $H=E_1$.

For the special case of a linear dissipation function, Eq. (6), we find the stationary solution:

$$\rho^0(q_1,\cdots q_f,p_1\cdots p_f)=Q^{-1}\exp\left(\frac{cH(2E_1-H)}{2D}\right). \tag{13}$$

In the limit of very strong pumping, $H\gg E_1$, this probability distribution reduces to a kind of microcanonical ensemble corresponding to the energy E_1.

The existence of exact solutions for the probability distribution, Eq. (12), allows one to derive several thermodynamic functions for the many-particle system, such as the *mean energy*,

$$U=Q^{-1}\int dHJ(H)H\exp\left(\int_0^H dH'\frac{g(H')}{D(H')}\right), \tag{14}$$

where the Jacobian $J(H)$ is defined by

$$dq_1\cdots dq_f dp_1\cdots dp_f=J(H)dH. \tag{15}$$

The *entropy* follows from the Gibbs formula, which yields here

$$S=+k_B\ln Q-k_B\int dHJ(H)\times\left[Q^{-1}\exp\left(\int_0^H\frac{g(H)}{D(H)}\right)\right]\int_0^H dH'\frac{g(H')}{D(H')}. \tag{16}$$

Further, the system has a Lyapunov functional K, which is provided by the Kullback entropy:

$$K[\rho,\rho^0]=\int dq_1\cdots dq_f dp_1\cdots dq_f\rho\ln\left(\frac{\rho}{\rho^0}\right). \tag{17}$$

This gives explicitly

$$K[\rho,\rho_0]=\ln Q-\frac{S}{k_B}+\left\langle\int_0^H\frac{g(H)}{D(H)}\right\rangle. \tag{18}$$

This functional is always nonincreasing.

If we want to generalize the description by means of the dissipative potential $G(I_0,I_1,I_2,\ldots)$ as used in Eq. (9), the situation is more difficult. But at least if the noise strength $D(H)$ is a constant ($D=\text{const}$), the corresponding Fokker-Planck equation

$$\frac{\partial\rho}{\partial t}+\sum p_i\frac{\partial\rho}{\partial q_i}-\sum\frac{\partial H}{\partial p_i}\frac{\partial\rho}{\partial p_i}=\sum\frac{\partial}{\partial p_i}\left[\frac{\partial G(I_0,I_1,I_2,\ldots)}{\partial p_i}\rho+D\frac{\partial\rho}{\partial p_i}\right] \tag{19}$$

is still solvable. Due to the invariant character of the I_k, the left-hand side of Eq. (19) disappears for all functions of I_k. Therefore, we have to search only for a function

$G(I_0,I_1,I_2,\ldots)$, for which also the collision term disappears. This way we find the stationary solution of Eq. (19):

$$\rho^0(q_1\cdots q_f,p_1\cdots p_f)=Q^{-1}\exp\left(-\frac{G(I_0,I_1,I_2\ldots)}{D}\right). \tag{20}$$

The derivative of ρ_0 vanishes if $G(I_0,I_1,I_2,\ldots)=\min$, which means that the probability is maximal on the attractor of the dissipative motion.

III. ENERGETIC CONDITIONS OF SWARMING

In this section, we want to apply the general description outlined above to swarm dynamics. Basically, at a certain level of abstraction a swarm can be viewed as a many-particle system with some additional coupling that would account for the typical correlated motion of the entities. In addition, also some energetic conditions must be satisfied in order to keep the swarm moving. Thus, *active motion* of the particles with a nonzero velocity is another basic ingredient for swarming. Since the conditions for active motion are dropped in many of the currently discussed swarm models [5,6,16], we first want to investigate the energetic conditions of swarming before turning to the second ingredient, coupling of individual motion.

A. Conditions for active motion

If we omit interactions between the particles, the Hamiltonian of the many-particle system is of the simple form

$$H=\sum_{i=1}^{N}H_i=\sum_{i=1}^{N}\frac{p_i^2}{2m}. \tag{21}$$

This allows one to reduce the description level from the N-particle distribution function to the one-particle distribution function,

$$\rho(q_1\cdots q_f,p_1\cdots p_f)=\prod_{i=1}^{N}\rho(\mathbf{r}_i,\mathbf{p}_i), \tag{22}$$

where the variable $\mathbf{r}_i$ is now used for the space coordinate of the particle i, and $\mathbf{p}_i$ stands for the momentum or, if $m=1$ is used in the following, for the *velocity* of the particle, respectively. The center of mass of the swarm is defined as

$$\mathbf{R}=\frac{1}{N}\sum\mathbf{r}_i, \tag{23}$$

whereas the mean momentum $\mathbf{P}$ and the mean angular momentum $\mathbf{L}$ are defined as

$$\mathbf{P}=\frac{1}{N}\sum\mathbf{p}_i, \tag{24}$$

$$\mathbf{L}=\frac{1}{N}\sum\mathbf{L}_i=\frac{1}{N}\sum\mathbf{r}_i\times\mathbf{p}_i. \tag{25}$$

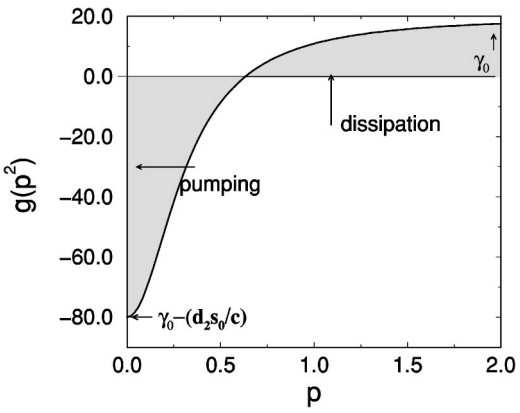

FIG. 1. Velocity-dependent dissipation function $g(p^2)$, Eq. (29) vs p. The velocity ranges for "pumping" $[g(p^2)<0]$ and "dissipation" $[g(p^2)>0]$ are indicated. Parameters: $s_0=10.0$, $\gamma_0=20.0$, $c=1.0$, $d_2=10.0$.

With $g(H)=g(p_i^2)$ and $D=\text{const}$, the Langevin Eq. (10) for each particle i reads, in the absence of an external potential,

$$\dot{\mathbf{r}}_i=\mathbf{p}_i,\quad \dot{\mathbf{p}}_i=-g(p_i^2)\mathbf{p}_i+(2D)^{1/2}\boldsymbol{\xi}_i(t), \tag{26}$$

where the strength D of the stochastic force results from the Einstein relation

$$D=\gamma_0 k_B T, \tag{27}$$

where T is the temperature and k_B is the Boltzmann constant.

For the dissipation function $g(p^2)$, we use again the general nonlinear ansatz of Eq. (7) in the limit of small values of β and finite A, Eq. (8). By means of the substitutions

$$(1+A)=c,\quad \gamma_1(1+A)=d_2 s_0,\quad \beta A=2d_2, \tag{28}$$

and with H of Eq. (21), Eq. (8) can be written in the form

$$g(p^2)=\gamma_0-\frac{s_0 d_2}{c+d_2 p^2}. \tag{29}$$

We note that all noninteracting systems with $g=g(p^2)$ are of canonical-dissipative type.

Equation (29) agrees with the velocity-dependent nonlinear friction function previously used in a model of active Brownian particles [30,31]. These are driven Brownian particles that move due to the influence of a stochastic force, but additionally are pumped with energy due to a velocity-dependent dissipation function $g(p^2)$, Eq. (29), which is plotted in Fig. 1.

The second term of the right-hand side (rhs) in Eq. (29), which results from the pumping of energy, has been physically substantiated in our earlier work [30,31]. We have assumed that the Brownian particles are able to take up energy from the environment at a constant rate s_0, which can be stored in an internal depot e. The internal energy can be converted to kinetic energy at a velocity-dependent rate $d(\mathbf{p})=d_2 p^2$, which results in an additional acceleration of the Brownian particle in the direction of movement. The value of the internal energy depot may be further decreased

due to internal dissipation processes, described by the constant c. Thus the resulting balance equation for the energy depot reads

$$\frac{de}{dt} = s_0 - ce(t) - d_2 p^2 e(t). \tag{30}$$

If we assume that the internal energy depot relaxes quickly compared to the motion of the particle, we find the quasistationary value

$$e_0 = \frac{s_0}{c + d_2 p^2}, \tag{31}$$

which eventually leads to the second term of the rhs in Eq. (29).

Depending on the parameters γ_O, d_2, s_0, c, the dissipation function, Eq. (29), may have a zero, where the friction is just compensated by the energy supply. It reads in the considered case

$$p_0^2 = v_0^2 = \frac{s_0}{\gamma_0} - \frac{c}{d_2}. \tag{32}$$

We see that for $p < p_0$, i.e., in the range of small momentums pumping due to negative friction occurs as an additional source of energy for the Brownian particle. Hence, slow particles are accelerated while the motion of fast particles is damped.

For $s_0 d_2 < \gamma_0 c$, we find no real-valued root of Eq. (32). This is the case of subcritical pumping, where the particle will move more or less like a simple Brownian particle. However, given the existence of a nonzero momentum p_0, i.e., for a supercritical pumping, the particle will be able to move in a ''high velocity'' or *active* mode [32,33], which displays several nontrivial features of motion, as will be shown by means of computer simulations in the next section.

B. Distribution function and dissipative potential

Due to the pumping mechanism discussed above, the conservation of energy clearly does not hold for the particle, i.e., we now have a nonequilibrium, canonical-dissipative system as discussed in Sec. II. This results in deviations from the known Maxwellian velocity distribution of an equilibrium canonical system.

As pointed out in Sec. II B, the probability density for the velocity $\rho(\mathbf{p},t)$ obeys the Fokker-Planck Equation (11), which reads, for the special case of the dissipation function, Eq. (29), and in the absence of an external potential,

$$\frac{\partial \rho(\mathbf{p},t)}{\partial t} = \frac{\partial}{\partial \mathbf{p}} \left[\left(\gamma_0 - \frac{d_2 s_0}{c + d_2 p^2} \right) \mathbf{p} \rho(\mathbf{p},t) + D \frac{\partial \rho(\mathbf{p},t)}{\partial \mathbf{p}} \right]. \tag{33}$$

We mention that Fokker-Planck equations with nonlinear friction functions are discussed in detail in [34].

The stationary solution of Eq. (33) is given by Eq. (20), which reads explicitly in the considered case

$$\rho^0(\mathbf{p}) = C_0 \exp\left(-\frac{G_0(p^2)}{D} \right), \tag{34}$$

$$= C_0 \left(1 + \frac{d_2 p^2}{c} \right)^{s_0/2D} \exp\left(-\frac{\gamma_0}{2D} p^2 \right), \tag{35}$$

where C_0 results from the normalization condition. $G_0(p^2)$ is the special form of the dissipation potential $G(I_0, I_1, I_2, \ldots)$ considering only $I_0 = H$ as the invariant of motion, and further H as given by Eq. (21). It reads explicitly

$$G(I_0) = G_0(p^2) = \gamma_0 \frac{p^2}{2} - \frac{s_0}{2} \ln\left(1 + \frac{d_2 p^2}{c} \right). \tag{36}$$

Compared to the Maxwellian velocity distribution of simple Brownian particles, a new prefactor appears now in Eq. (35) that results from the additional pumping of energy. For a subcritical pumping, $s_0 d_2 < c\gamma_0$, where we do not find a real-valued root of the dissipation function, Eq. (29), only a *unimodal velocity distribution* results, centered around the maximum $\mathbf{p}_0 = 0$. However, for supercritical pumping, $s_0 d_2 > c\gamma_0$, if the root of $g(p^2)$ is real, we find a *craterlike velocity distribution*, which indicates strong deviations from the Maxwell distribution [35].

This is also shown in Fig. 2, which presents computer simulations of the velocity distribution of 10 000 particles after a sufficiently long time [only the x dimension of the two-dimensional (2D) simulation is shown]. For the supercritical case, two distinct peaks of the velocity distribution are found at $p_x = \{-0.63, +0.63\}$. The values of these maxima agree with the deterministic result for the stationary velocity, Eq. (32).

We note that non-Maxwellian velocity distributions for active motion have also been observed experimentally in cells, such as granulocytes [36,37].

C. Mean squared displacement and stationary values

As Fig. 2 shows, the momentum distribution is centered around $\mathbf{p} = 0$ both for subcritical and supercritical pumping. If we consider a nearly spherical swarm of particles in the two-dimensional space $\mathbf{r} = \{x, y\}$ as in the computer simulations in this section, its center of mass, Eq. (23), and mean momentum, Eq. (24), will come to rest. Thus they are not affected by the pumping, but other quantities are, such as the mean squared displacement,

$$\Delta R^2(t) = \left\langle \left(\frac{1}{N} \sum \left[\mathbf{r}_i(t) - \mathbf{r}_i(0) \right] \right)^2 \right\rangle. \tag{37}$$

In the limit of pure Brownian motion, it is known that the mean squared displacement increases in time as

$$\Delta R^2(t) = 4 D_r t, \tag{38}$$

where $D_r = k_B T / \gamma_0 = D / \gamma_0^2$ is the spatial diffusion coefficient. Thus, Eq. (38) will be the lower limit for subcritical pumping of the particles. On the contrary, in the case of

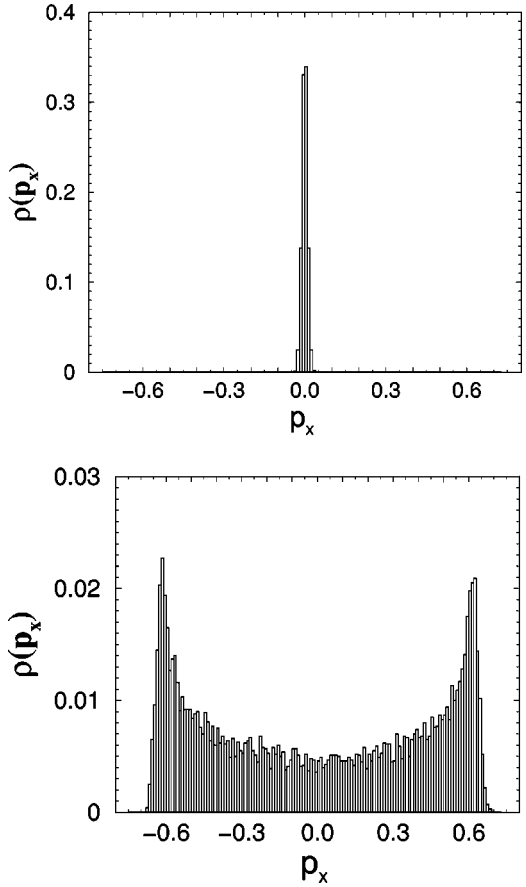

FIG. 2. Velocity distribution $\rho(p_x)$ for a swarm of 10 000 particles at $t=1000$ (i.e., in the stationary regime). Only p_x of the 2D simulation is shown. Top, subcritical pumping $d_2=1.0$; bottom, supercritical pumping, $d_2=10.0$. Other parameters: $D=10^{-3}$, $s_0=10.0$, $\gamma_0=20.0$, $c=1.0$. Initial conditions: $\mathbf{r}_i(0)=\{0.0,0.0\}$, $\mathbf{p}_i(0)=\{0.0,0.0\}$ for all particles.

supercritical pumping it has been shown [35,38] that the mean squared displacement will grow in time approximately as

$$\Delta R^2(t)=\frac{2v_0^4}{D}t, \tag{39}$$

where v_0 is given by Eq. (32). Consequently, the diffusion coefficient D_r in Eq. (38) for the case of supercritical pumping has to be replaced by an *effective* spatial diffusion coefficient,

$$D_r^{\text{eff}}=\frac{v_0^2}{2D}=\frac{1}{2D}\left(\frac{s_0}{\gamma_0}-\frac{c}{d_2}\right). \tag{40}$$

This result holds for noninteracting particles in the limit of relatively weak noise intensity D and/or strong pumping and will therefore give an upper limit for $\Delta R^2(t)$. We note the high sensitivity with respect to noise expressed in the scaling with $(1/D)$.

Figure 3 shows the mean squared displacement of a swarm of 2000 particles for the case of both subcritical and supercritical pumping, together with the theoretical results of

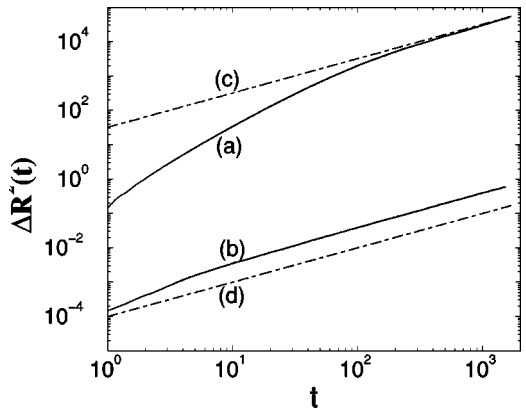

FIG. 3. Mean squared displacement $\Delta R^2(t)$, Eq. (37) of a swarm of 2000 particles as a function of time. (a) Supercritical pumping, $d_2=10.0$, (b) subcritical pumping, $d_2=1.0$. $D=10^{-2}$, for the other parameters and the initial conditions see Fig. 2. The additional curves give the theoretical results of Eq. (39) (c) (upper limit) and Eq. (38) (d) (lower limit).

Eqs. (38) and (39). We see that for long times the computer simulations for supercritical pumping agree very well with Eq. (39).

Another quantity affected by the sub/supercritical pumping is the stationary velocity $p_0^2=v_0^2$, Eq. (32). In two dimensions, these stationary velocities define a cylinder, $p_x^2+p_y^2=p_0^2$, in the four-dimensional state space $\{x,y,p_x,p_y\}$ that attracts all deterministic trajectories of the dynamic system [35]. Figure 4 shows the results of computer simulations for $p^2(t)$ for the case of supercritical pumping. The convergence toward the theoretical result, Eq. (32), can be clearly observed.

IV. GLOBALLY COUPLED SWARMS

So far we have neglected any coupling within the many-particle ensemble. This leads to the effect that the swarm eventually disperses in the course of time, whereas a ''real'' swarm would maintain its coherent motion. A common way

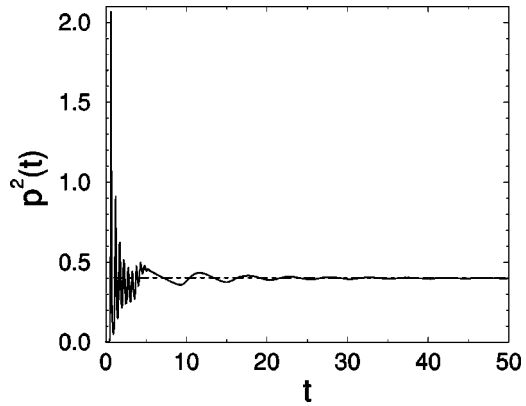

FIG. 4. Averaged squared velocity $p^2(t)=1/N\Sigma p_i^2(t)$, Eq. (26), of a swarm of 2000 particles as a function of time. $D=10^{-4}$, for the other parameters and the initial conditions; see Fig. 2. The dash-dotted line gives the stationary velocity, Eq. (32).

to introduce correlations between the moving particles in physical swarm models is the coupling to a mean value. For example, in [1,2] the coupling of the particles' individual *orientations* (i.e., direction of motion) to the mean orientation of the swarm is discussed. Other versions assume the coupling of the particles' velocities to a *local average velocity*, which is calculated over a space interval around the particle [2,6].

A. Coupling to the center of mass

In this paper, we are mainly interested in *global* couplings of the swarm, which fit it into the theory of canonical-dissipative systems outlined in Sec. II. As the simplest case, we may first discuss the global coupling of the swarm to the *center of mass*, Eq. (23). That means the particle's position $\mathbf{r}_i$ is related to the mean position of the swarm $\mathbf{R}$ via a potential $U(\mathbf{r}_i,\mathbf{R})$. For simplicity, we may assume a parabolic potential

$$U(\mathbf{r}_i,\mathbf{R})=\frac{a}{2}(\mathbf{r}-\mathbf{R})^2. \tag{41}$$

The harmonic potential generates a force directed to the center of mass that can be used to control the dispersion of the swarm. It reads, in the case considered,

$$\nabla U(\mathbf{r})=a(\mathbf{r}_i-\mathbf{R})=\frac{a}{N}\sum_{j=1}^{N}(\mathbf{r}_i-\mathbf{r}_j), \tag{42}$$

With Eq. (42), the corresponding Langevin Eq. (26) of the many-particle system reads explicitly

$$\dot{\mathbf{p}}_i=-g(p_i^2)\mathbf{p}_i-\frac{a}{N}\sum_{j=1}^{N}(\mathbf{r}_i-\mathbf{r}_j)+(2D)^{1/2}\boldsymbol{\xi}_i(t). \tag{43}$$

Hence, in addition to the dissipation function there is now an attractive force between each two particles i and j that depends linearly on the distance between them. With respect to the harmonic interaction potential Eq. (41), we call such a swarm a *harmonic* swarm [39].

Strictly speaking, the dynamical system of Eq. (43) is not a canonical-dissipative one, but as shown in [31] it may be reduced to this type by some approximations, which will also be discussed below. We note that this kind of swarm model has been previously investigated in [3] for the one-dimensional case, but with a different dissipation function $g(p^2)$, for which we use Eq. (29) again. Obviously, as shown in Sec. III B, swarming will occur only for supercritical conditions.

With the assumed coupling to the center of mass $\mathbf{R}$, the motion of the swarm can be considered as a superposition of two motions: (i) the motion of the center of mass itself, and (ii) the motion of the particles relative to the center of mass. Taking into account that the noise acting on the different particles is not correlated, the center of mass for the assumed coupling obeys a force-free motion,

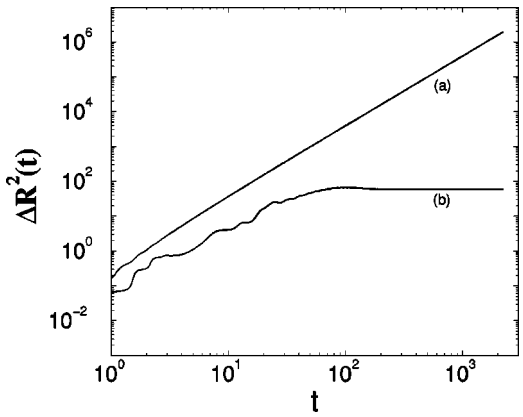

FIG. 5. Mean squared displacement $\Delta R^2(t)$, Eq. (37) of a swarm of 2000 particles coupled to the center of mass. Initial conditions: $\mathbf{r}_i(0)=\{0.0,0.0\}$, (a) $\mathbf{p}_i(0)=\{1.0,1.0\}$, (b) $\mathbf{p}_i(0)=\{0.0,0.0\}$, for all particles. Parameters: $a=1$, $D=10^{-8}$, $d_2=10.0$, $s_0=10.0$, $\gamma_0=20.0$, $c=1.0$.

$$\dot{\mathbf{R}}=\mathbf{P}, \quad \dot{\mathbf{P}}=-\frac{1}{N}\sum_{i=1}^{N}g(p_i^2)\mathbf{p}_i \tag{44}$$

Because of the nonlinearities in the dissipation function $g(p^2)$ both motions (i) and (ii) cannot be simply separated. The term $g(p^2)$ vanishes only for two cases: the trivial one that is free motion without dissipation/pumping, or the case of supercritical pumping where $p_i^2=p_0^2$, Eq. (32) for each particle. Then, the mean momentum becomes an invariant of motion, $\mathbf{P}(t)=\mathbf{P}_0=\text{const}$ and the center of mass moves according to $\mathbf{R}(t)=\mathbf{R}(0)+\mathbf{P}_0(t)$. This behavior may also critically depend on the initial conditions of the particles, $\mathbf{p}_i(0)$, and shall be investigated in more detail now.

In [3] an approximation for the mean velocity $\mathbf{P}(t)$ of the swarm in one dimension is discussed that shows the existence of two different asymptotic solutions depending on the noise intensity D and the initial momentum $\mathbf{p}_i(0)$ of the particles. Below a critical noise intensity D_c, the initial condition $p_i^2(0)>p_0^2$ leads to a swarm the center of which travels with a constant nontrivial mean velocity, while for the initial condition $p_i^2(0)<p_0^2$ the center of the swarm is at rest.

We can confirm these findings by means of two-dimensional computer simulations presented in Figs. 5 and 6, which show the mean squared displacement, the average squared velocity of the swarm, and the squared mean velocity of the center of mass for the two different initial conditions.

For (a) $p_i^2(0)>p_0^2$ we find a continuous increase of $\Delta R^2(t)$ [Fig. 5(a)], while the velocity of the center of mass reaches a constant value: $P^2(t)=[N^{-1}\Sigma_i\mathbf{p}_i(t)]^2\rightarrow p_0^2$, known as the stationary velocity of the force-free case, Eq. (32). The average squared velocity reaches a constant nontrivial value, too, which depends on the noise intensity and the initial conditions, $p_i^2(0)>p_0^2$, i.e., on the energy initially supplied (cf. Fig. 6 top).

For (b) $p_i^2(0)<p_0^2$ we find that the mean squared displacement after a transient time reaches a constant value, i.e., the center of mass comes to rest [Fig. 5(b)], which corre-

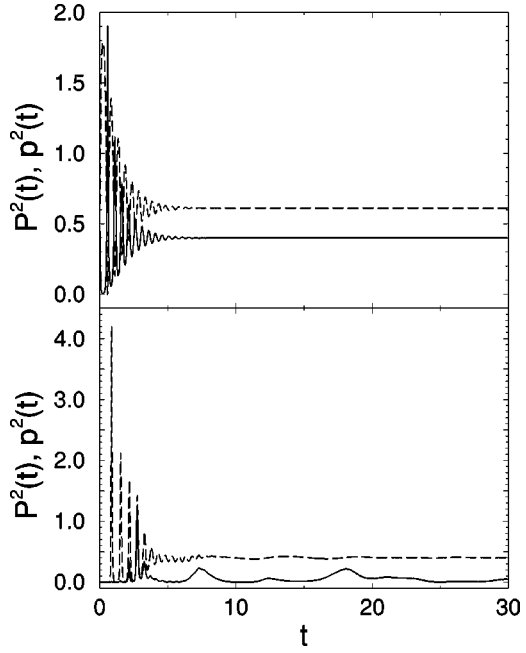

FIG. 6. Squared velocity of the center of mass, $P^2(t) = [N^{-1}\Sigma_i \mathbf{p}_i(t)]^2$ (solid lines) and averaged squared velocity $p^2(t) = N^{-1}\Sigma p_i^2(t)$ (dashed lines) for the simulations shown in Fig. 5: (top) initial conditions (a), (bottom) initial conditions (b).

sponds to $P^2(t) \to 0$ in Fig. 6 (bottom). In this case, however, the average squared velocity of the swarm reaches the known stationary velocity, $p^2(t) = 1/N\Sigma p_i^2(t) \to p_0^2$. Consequently, in this case the energy provided by the pumping goes into the motion *relative to the center of mass* while the motion of the center of mass is damped out (cf. also [39]). Thus, in the following we want to investigate the relative motion of the particles in more detail.

Using relative coordinates, $\{x_i, y_i\} \equiv \mathbf{r}_i - \mathbf{R}$, the dynamics of each particle in the two-dimensional space is described by four coupled first-order differential equations:

$$\dot{x}_i = p_{xi} - P_x,$$

$$\dot{p}_{xi} - \dot{P}_x = -g(p_i^2)p_{xi} - ax_i + (2D)^{1/2}\xi_i(t),$$

$$\dot{y}_i = p_{yi} - P_y,$$

$$\dot{p}_{yi} - \dot{P}_y = -g(p_i^2)p_{yi} - ay_i + (2D)^{1/2}\xi_i(t). \qquad (45)$$

For $\mathbf{P} = 0$, i.e., for the initial conditions $p_i^2 < p_0^2$ and sufficiently long times, this dynamics is equivalent to the motion of free (or uncoupled) particles in a parabolic potential $U(x,y) = a(x^2 + y^2)/2$ with the origin {0, 0}. Thus, within this approximation the system becomes a canonical-dissipative system again, in the strict sense used in Sec. II.

Figure 7 presents computer simulations of Eq. (45) for the relative motion of the particle swarm in the parabolic potential [43]. (Note that in this case all particles started from the same position slightly *outside* the origin of the parabolic potential. This has been chosen in order to make the evolution of the different branches more visible.) As the snapshots of

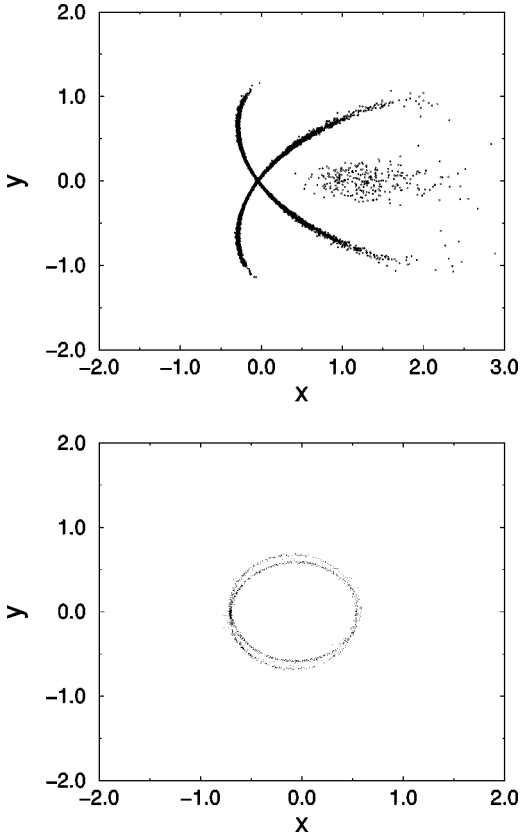

FIG. 7. Snapshots (relative coordinates) of a swarm of 10 000 particles moving according to Eq. (45) with $\mathbf{P} = 0$, (top) $t = 15$, (bottom) $t = 99$. Initial conditions: $\{x_i, y_i\} = \{0.5, 0.0\}$, $\{p_{xi}, p_{yi}\} = \{0.0, 0.0\}$ for all particles. Parameters: $a = 1$, $D = 10^{-5}$, $s_0 = 10.0$; $c = 1.0$; $\gamma_0 = 20$, $d_2 = 10$.

the spatial dispersion of the swarm show, we find after an initial stage the occurrence of two branches of the swarm that results from a *spontaneous symmetry break* (cf. Fig. 7 top). These two branches will, after a sufficiently long time, move on two limit cycles (as already indicated in Fig. 7 bottom). One of these limit cycles refers to the left-handed, the other one to the right-handed direction of motion in the 2D space. This finding also agrees with the the theoretical investigations of the deterministic case [31] that showed the existence of a limit cycle with the amplitude

$$r_0 = |p_0| a^{-1/2}, \qquad (46)$$

provided the relation $s_0 d_2 > \gamma_0 c$ is fulfilled. In the small noise limit the radius of the limit cycles shown in Fig. 7 agrees with the value of r_0. Further, Fig. 6 has shown that the average squared velocity $p^2(t)$ of the swarm indeed approaches the theoretical value of Eq. (32).

The existence of two opposite rotational directions of the swarm can be also clearly seen from the distribution of the angular momenta L_i of the particles. Figure 8 shows the existence of a bimodal distribution for $\rho(L)$. (The observant reader may notice that each of these peaks actually consists of two subpeaks resulting from the initial conditions, which are still not forgotten at $t = 99$.) Each of the main peaks is centered around the theoretical value

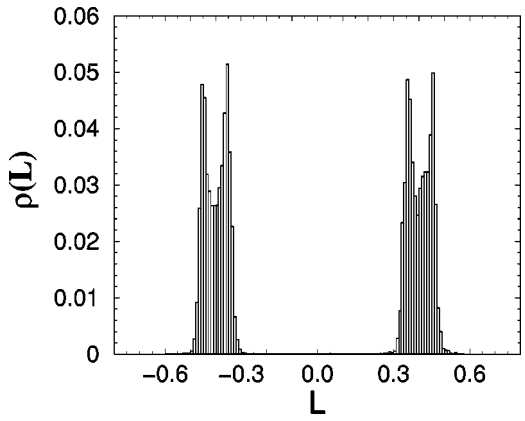

FIG. 8. Angular momentum distribution $\rho(L)$ for a swarm of 10 000 particles at $t=99$. The figure refers to the spatial snapshot of the swarm shown in Fig. 7 (bottom).

$$|\mathbf{L}| = L_0 = r_0 p_0, \tag{47}$$

where r_0 is given by Eq. (46) and p_0 is given by Eq. (32).

The emergence of the two limit cycles means that the dispersion of the swarm is kept within certain spatial boundaries. This occurs after a transient time used to establish the correlation between the individual particles. In the same manner as the motion of the particles becomes correlated, the motion of the center of mass is slowed down until it comes to rest, as already shown in Fig. 6.

This, however, is not the case if the initial conditions $p_i^2(0) > p_0^2$ are chosen. Then, the energy provided by the pumping does not go completely into the relative motion of the particles and the establishment of the limit cycles as discussed above. Instead, the center of mass keeps moving as shown in Fig. 5, while the swarm itself does not establish an internal order. Figure 9 displays a snapshot of the relative positions of the particles in this case (note the different scales of the axes compared to Fig. 7).

B. Coupling via mean momentum and mean angular momentum

In the following we want to discuss two other ways of *global* coupling of the swarm that fit into the general frame-

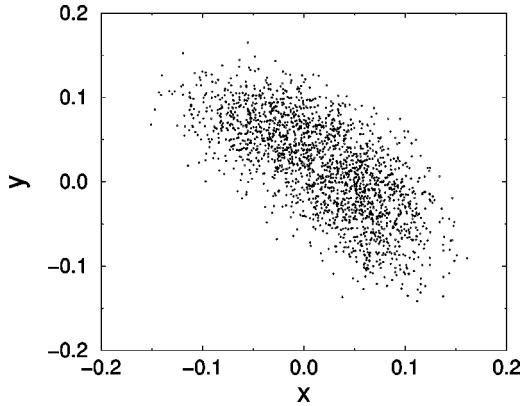

FIG. 9. Snapshot (relative coordinates) of a swarm of 10 000 particles moving according to Eq. (45) at $t=99$. Initial conditions: $\{x_i, y_i\} = \{0.5, 0.0\}$, $\{p_{xi}, p_{yi}\} = \{1.0, 1.0\}$ for all particles. Parameters see Fig. 7.

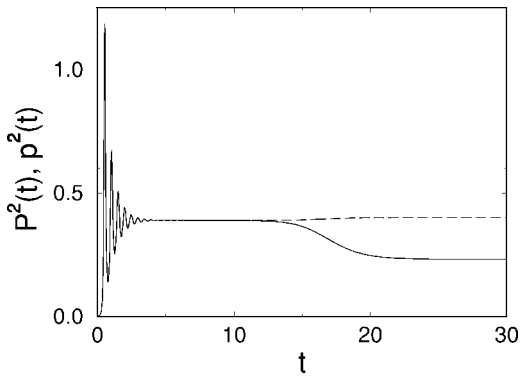

FIG. 10. Squared velocity of the center of mass, $P^2(t) = [N^{-1}\Sigma_i \mathbf{p}_i(t)]^2$ (solid lines) and averaged squared velocity $p^2(t) = N^{-1}\Sigma p_i^2(t)$ (dashed lines) for the simulations shown in Fig. 11.

work of canonical-dissipative systems outlined in Sec. II. There, we have introduced a dissipative potential $G(I_0, \mathbf{I}_1, \mathbf{I}_2, \ldots)$ that depends on the different invariants of motion $\mathbf{I}_i$. So far, we have only considered $I_0 = H$, Eq. (21) in the swarm model. If we additionally include the mean momentum $\mathbf{I}_1 = \mathbf{P}$, Eq. (24) as the first invariant of motion, the dissipative potential may read

$$G(I_0, \mathbf{I}_1) = \sum_{i=1}^{N} G_0(p_i^2) + G_1(\mathbf{P}), \tag{48}$$

$$G_1(\mathbf{P}) = \frac{C_P}{2}\left(\sum_{i=1}^{N} p_i - N\mathbf{P}_1 \right)^2. \tag{49}$$

Here, $G_0(p^2)$ is given by Eq. (36). The stationary solution of the probability distribution, $\rho^0(\mathbf{p})$ is again given by Eq. (20). In the absence of an external potential $U(\mathbf{r})$, the Langevin equation that corresponds to the dissipation potential of Eq. (48) now reads

$$\dot{\mathbf{r}}_i = \mathbf{p}_i$$

$$\dot{\mathbf{p}}_i = -g(p_i^2)\mathbf{p}_i - C_P\left(\sum \mathbf{p}_i - N\mathbf{P}_1 \right) + (2D)^{1/2}\boldsymbol{\xi}_i(t). \tag{50}$$

The term $G_1(\mathbf{P})$ is so chosen that it may drive the system towards the prescribed momentum $\mathbf{P}_1$, where the relaxation time is proportional to C_P^{-1}. If we have a vanishing dissipation function, i.e., $g=0$ for $p_i^2 = p_0^2$, it follows from Eq. (50) for the mean momentum

$$\mathbf{P}(t) = \frac{1}{N}\sum_{i=1}^{N} \mathbf{p}_i(t) = \mathbf{P}_1 + [\mathbf{P}(0) - \mathbf{P}_1]e^{-C_p t}. \tag{51}$$

The existence of two terms G_0 and G_1, however, could lead to competing influences of the resulting forces, and a more complex dynamics of the swarm results. As before, this may also depend on the initial conditions, i.e., $P_1^2 \geqslant p_0^2$ or $P_1^2 \leqslant p_0^2$.

Figure 10 shows the squared velocity of the center of mass, $P^2(t)$ and the average squared velocity of the swarm

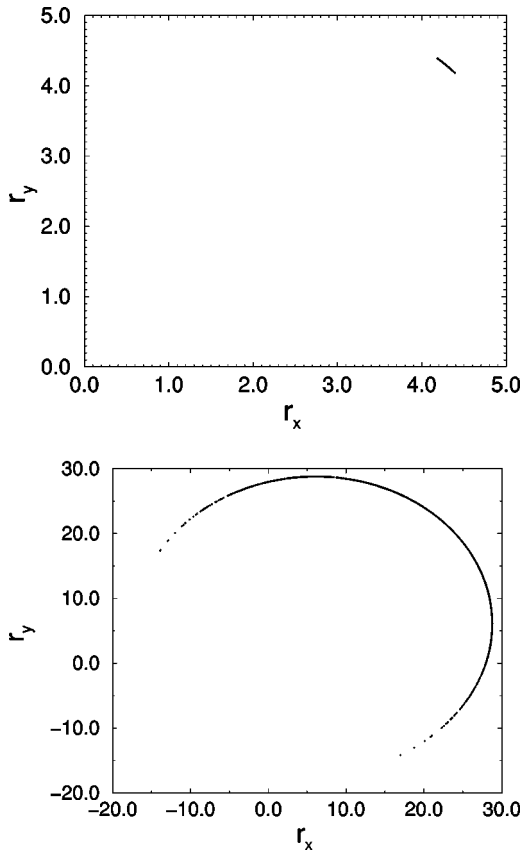

FIG. 11. Snapshots of a swarm of 2000 particles moving according to Eq. (50). (top) $t=10$, (bottom) $t=50$. Initial conditions: $\{r_{xi},r_{yi}\}=\{0.0,0.0\}$, $\{p_{xi},p_{yi}\}=\{0.0,0.0\}$ for all particles. Parameters: $\{P_{1x},P_{1y}\}=\{0.344,0.344\}$, $C_p=10^{-3}$ $D=10^{-8}$, $s_0=10.0$; $c=1.0$; $\gamma_0=20$, $d_2=10$.

$p^2(t)$ for $P_1^2\leqslant p_0^2$, We find an intermediate stage, where both velocities are equal, before the global coupling drives the mean momentum $\mathbf{P}$ towards the prescribed value $\mathbf{P}_1$, i.e., $P^2(t)\rightarrow(P_{1x}^2+P_{1y}^2)$. On the other hand, $p^2(t)\rightarrow p_0^2$, as we have found before for the force-free case and for the linearly coupled case for similar initial conditions. The noticeable decrease of P^2 after the initial time lag can be best understood by looking at the spatial snapshots of the swarm provided in Fig. 11. For $t=10$, we find a rather compact swarm where all particles move into the same (prescribed) direction. For $t=50$, the correlations between the particles have already become effective, which means the swarm begins to establish a circular front, which, however, does not become a full circle [44]. Eventually, we find again that the energy provided by the pumping goes into the motion of the particles relative to the center of mass, while the motion of the center of mass itself is driven by the prescribed momentum.

For the initial condition $P_1^2\geqslant p_0^2$ the situation is different again, as Fig. 12 shows. Apparently, both curves are the same for a rather small noise intensity, i.e., $P^2(t)=p^2(t)$ are both equal, but different from p_0^2, Eq. (32), and the prescribed momentum P_1^2. This can be only realized if all particles move in parallel in the same direction. Thus, a snapshot of the swarm would much look like the top part of Fig. 11.

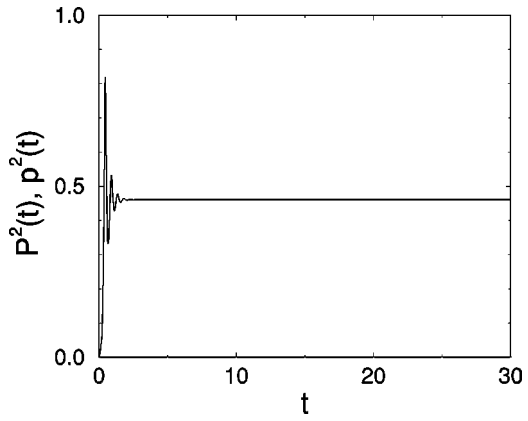

FIG. 12. Squared velocity of the center of mass, $P^2(t)=[N^{-1}\Sigma_i\mathbf{p}_i(t)]^2$ (solid lines) and averaged squared velocity $p^2(t)=N^{-1}\Sigma p_i^2(t)$ (dashed lines) for a swarm of 2000 particles moving according to Eq. (50). $\{P_{1x},P_{1y}\}=\{1.0,1.0\}$, for the other parameters and initial conditions see Fig. 11.

Eventually, we may also use the second invariant of motion, $\mathbf{I}_2=\mathbf{L}$, Eq. (25), for a global coupling of the swarm. In this case, the dissipative potential may be defined as follows:

$$G(I_0,\mathbf{I}_2)=\sum_{i=1}^{N}G_0(p_i^2)+G_2(\mathbf{L}), \tag{52}$$

$$G_2(\mathbf{L})=\frac{C_L}{2}\left(\sum\ \mathbf{r}_i\times\mathbf{p}_i-N\mathbf{L}_1\right)^2, \tag{53}$$

where $G_0(p^2)$ is again given by Eq. (36). The term $G_2(\mathbf{L})$ shall drive the system to a prescribed angular momentum $\mathbf{L}_1$ with a relaxation time proportional to C_L^{-1}.

$\mathbf{L}_1$ can be used to break the symmetry of the swarm towards a prescribed rotational direction. In Sec. IV A we observed the spontaneous occurrence of left-hand and right-hand rotations of a swarm of linearly coupled particles. Without an additional coupling, both rotational directions are equally probable in the stationary limit. Considering both the parabolic potential $U(\mathbf{r},\mathbf{R})$, Eq. (41), and the dissipative potential, Eq. (52), the corresponding Langevin equation may now read

$$\dot{\mathbf{r}}_i=\mathbf{p}_i$$

$$\dot{\mathbf{p}}_i=-g(p_i^2)\mathbf{p}_i-\frac{a}{N}\sum_{j=1}^{N}(\mathbf{r}_i-\mathbf{r}_j)+C_L\mathbf{r}_i\times\left(\sum\ \mathbf{r}_i\times\mathbf{p}_i-N\mathbf{L}_1\right)$$
$$+(2D)^{1/2}\boldsymbol{\xi}_i(t). \tag{54}$$

The computer simulations shown in Fig. 13 clearly display a unimodal distribution of the angular momenta L_i of the particles, which can be compared to Fig. 8 without coupling to the angular momentum. Consequently, we find in the long time limit only one limit cycle corresponding to the movement of the swarm into the same rotational direction. The radius r_0 of the limit cycle is again given by Eq. (46).

We would like to add that also in this case the dynamics depends on the initial condition $\mathbf{L}_1$. For simplicity, we have

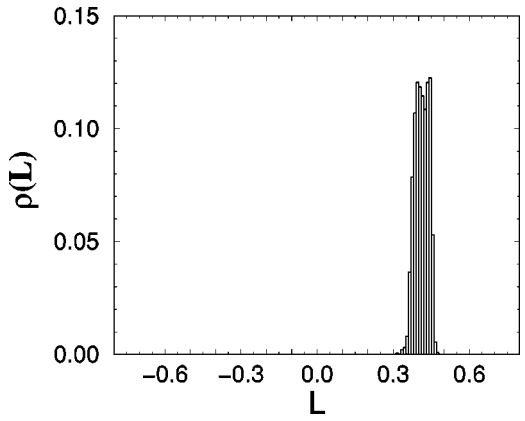

FIG. 13. Angular momentum distribution $\rho(L)$ for a swarm of 2000 particles at $t=99$. For comparison with Fig. 8, the parameters, initial conditions and snapshot times are the same as in Fig. 7. Additional coupling: $C_L=0.05$, $\{L_{1z}\}=\{0.4\}$.

assumed here $|\mathbf{L}_1|=L_0=r_0p_0$, Eq. (47) which is also reached by the mean angular momentum L in the course of time (cf. Fig. 13). For initial conditions $|\mathbf{L}_1|\ll L_0$, there is of course no need for the rotation of *all* particles in the same direction. Hence we observe both left- and right-handed rotations of the particles with different shares, so that the mean angular momentum is still $\mathbf{L}\rightarrow\mathbf{L}_1$. This results in a broader distribution of the angular momenta of the particles instead of the clear unimodal distribution shown in Fig. 13. For initial conditions $|\mathbf{L}_1|\gg L_0$, on the other hand, the stable rotation of the swarm breaks down after some time, since the driving force $\mathbf{L}\rightarrow\mathbf{L}_1$ tends to destabilize the attractor $\mathbf{L}\rightarrow\mathbf{L}_0$. This effect will be investigated in a forthcoming paper, together with some combined effects of the different global couplings.

V. DISCUSSION

Finally, we can also combine the different global couplings discussed above by defining the dissipation potential as

$$G(I_0,\mathbf{I}_1,\mathbf{I}_2)=G(p^2,\mathbf{P},\mathbf{L})=G_0(p^2)+G_1(\mathbf{P})+G_2(\mathbf{L}). \tag{55}$$

$G_0(p^2)$ is given by Eq. (36), $G_1(\mathbf{P})$ by Eq. (49) and $G_2(\mathbf{L})$ by Eq. (53). Considering further an additional—external or interaction—potential, the corresponding Langevin equation can be written in the more general form

$$\dot{\mathbf{r}}_i=\mathbf{p}_i,$$

$$\dot{\mathbf{p}}_i=-g(p_i^2)\mathbf{p}_i-\frac{\partial}{\partial r_i}[\alpha_0U(\mathbf{r},\mathbf{R})]-\frac{\partial}{\partial p_i}[\alpha_1(\mathbf{P}-\mathbf{P}_1)^2+\alpha_2(\mathbf{L}-\mathbf{L}_1)^2]+(2D)^{1/2}\boldsymbol{\xi}_i(t). \tag{56}$$

The mean momentum $\mathbf{P}$ and mean angular momentum $\mathbf{L}$ are given by Eqs. (24) and (25), whereas the constant vectors $\mathbf{P}_1$ and $\mathbf{L}_1$ are used to break the spatial or rotational symmetry of the motion toward a preferred direction. The different constants α_i may determine whether or not the respective influence of the conservative or dissipative potential is effective. They further determine the time scale when the global coupling becomes effective. The term $g(p^2)$, Eq. (29), on the other hand, considers the energetic conditions for the active motion of the swarm, i.e., it determines whether the particle of the swarm is able to ''take off'' at all.

The combination of the different types of coupling may lead to a rather complex swarm dynamics, as already indicated in the examples discussed in this paper. In particular, we note that the different terms may have competing influences on the swarm, which would then lead to a ''frustrated'' dynamics with many possible attractors.

In this paper, we have basically restricted the investigation of the swarm dynamics to global couplings that fit into (or can be reduced within some approximations to) the general outline of canonical-dissipative systems. Finally, we want to add some comments on that. On one hand, it is possible to extend this kind of approach to other invariants of motion, thereby, e.g., covering previous investigations of swarms coupled via the mean orientation of the particles [1,2]. On the other hand, we want to emphasize that canonical-dissipative systems are a theoretical class of models, where *both* conservative and dissipative elements of the dynamics are determined by invariants of the mechanical motion. Thus, from this perspective, a more realistic swarm dynamics may be also based on less restrictive assumptions.

The advantage of using canonical-dissipative systems as a framework for swarm dynamics is given by the fact that in many cases the rather complex dynamics can be mapped to an analytically tractable model. With the Hamiltonian theory of many-particle systems as a starting point, we are able to extend known solutions for conservative systems to nonconservative systems. This allows us to construct a canonical-dissipative system, the solutions of which converge to the solution of the conservative system with given energy. That means that for given initial conditions, we can predict the asymptotic solution of the canonical-dissipative dynamics by means of the solutions of the Hamiltonian equations on the respective energy surfaces.

In addition to these theoretical considerations that have a value of their own, we want to note that the framework of canonical-dissipative systems still covers important features of real (biological) systems, such as energy takeup and dissipation. The general description outlined in this paper allows us to gradually add more and more complexity to the swarm model, thereby bridging the gap between a known (physical) dynamics and a more complex (biological) dynamics [39,40]. Some hints for this shall be given at the end.

On the level of the ''individual'' particles, the key dynamics of the model is given by a modified Langevin equation that, in addition to stochastic influences, also considers other forces on the particle, resulting, e.g., from external potentials, interactions, use of stored energy [31], or influences of a self-consistent field [7,8] that already exceed the framework of canonical-dissipative systems.

The consideration of an *external* potential also allows one to model the *spatial environment* of the swarm, for instance

to consider *obstacles* [30]. Additionally, we can also consider that the pumping of energy for the particles is restricted to certain spatial domains that model *food sources*. In this case the dissipation function $g(H)$ also becomes a spatial function. Such an extension has been already discussed in [30,41] and can also be implemented in the swarm model discussed here. Finally, we note that the genuine particle-based approach to collective phenomena used in this paper is not restricted to biological systems, but is also applicable for describing and simulating complex interactive systems in a wide range of applications, even in economics and social systems [42].

ACKNOWLEDGMENTS

The authors thank J. Dunkel and U. Erdmann for discussions.

[1] A. Czirok, E. Ben-Jacob, I. Cohen, and T. Vicsek, Phys. Rev. E **54**, 1791 (1996).
[2] A. Czirok and T. Vicsek, Physica A **281**, 17 (2000).
[3] A. Mikhailov and D. H. Zanette, Phys. Rev. E **60**, 4571 (1999).
[4] J. Toner and Y. Tu, Phys. Rev. Lett. **75**, 4326 (1995).
[5] T. Vicsek, A. Czirok, E. Ben-Jacob, I. Cohen, and O. Shochet, Phys. Rev. Lett. **75**, 1226 (1995).
[6] A. Czirok, A. L. Barabasi, and T. Vicsek, Phys. Rev. Lett. **82**, 209 (1999).
[7] L. Schimansky-Geier, M. Mieth, H. Rosé, and H. Malchow, Phys. Lett. A **207**, 140 (1995).
[8] L. Schimansky-Geier, F. Schweitzer, and M. Mieth, in *Self-Organization of Complex Structures: From Individual to Collective Dynamics*, edited by F. Schweitzer (Gordon and Breach, London, 1997), pp. 101–118.
[9] A. Stevens, J. Biol. Systems **3**, 1059 (1995).
[10] E. Ben-Jacob, O. Shochet, I. Cohen, A. Czirok, and T. Vicsek, Phys. Rev. Lett. **75**, 2899 (1995).
[11] T. Höfer, J. A. Sherratt, and P. K. Maini, Proc. R. Soc. London, Ser. B **259**, 249 (1995).
[12] V. Calenbuhr and J. L. Deneubourg, in *Biological Motion*, edited by W. Alt and G. Hoffmann (Springer, Berlin, 1990), pp. 453–469.
[13] L. Edelstein-Keshet, J. Math. Biol. **32**, 303 (1994).
[14] F. Schweitzer, K. Lao, and F. Family, BioSystems **41**, 153 (1997).
[15] M. Schienbein and H. Gruler, Phys. Rev. E **52**, 4183 (1995).
[16] E. V. Albano, Phys. Rev. Lett. **77**, 2129 (1996).
[17] D. Helbing and T. Vicsek, New J. Phys. **1**, 13 (1999).
[18] R. Graham, in *Quantum Statistics in Optics and Solid State Physics*, edited by G. Höhlen, Springer Tracts in Modern Physics Vol. 66 (Springer, Berlin, 1973), p. 111.
[19] H. Haken, Z. Phys. **273**, 267 (1973).
[20] M. O. Hongler and D. M. Ryter, Z. Phys. B **31**, 333 (1978).
[21] W. Ebeling and H. Engel-Herbert, Physica A **104**, 378 (1980).
[22] W. Ebeling, in *Chaos and Order in Nature*, edited by H. Haken, Springer Series in Synergetics Vol. 11 (Springer, Berlin, 1981), p. 188.
[23] R. Feistel and W. Ebeling, *Evolution of Complex Systems: Self-Organization, Entropy and Development* (Kluwer, Dordrecht, 1989).
[24] W. Ebeling, in *Stochastic Processes in Physics, Chemistry and Biology*, edited by J. A. Freund and T. Pöschel, Lecture Notes in Physics Vol. 557 (Springer, Berlin, 2000), pp. 390–399.
[25] A. A. Andronov, A. A. Witt, and S. Chaikin, *Theorie der Schwingungen* (Akademie-Verlag, Berlin, 1965), Vol. I; *Theorie der Schwingungen* (Akademie-Verlag, Berlin, 1969), Vol. II.
[26] V. Makarov, W. Ebeling, and M. Velarde, Int. J. Bifurcation Chaos Appl. Sci. Eng. **10**, 1075 (2000).
[27] M. Toda, *Theory of Nonlinear Lattices* (Springer, Berlin, 1981).
[28] M. Toda, *Nonlinear Waves and Solitons* (Kluwer, Dordrecht, 1983).
[29] W. Ebeling, Condens. Matter Phys. **3**, 285 (2000).
[30] F. Schweitzer, W. Ebeling, and B. Tilch, Phys. Rev. Lett. **80**, 5044 (1998).
[31] W. Ebeling, F. Schweitzer, and B. Tilch, BioSystems **49**, 17 (1999).
[32] B. Tilch, F. Schweitzer, and W. Ebeling, Physica A **273**, 294 (1999).
[33] F. Schweitzer, B. Tilch, and W. Ebeling, Eur. Phys. J. B **14**, 157 (2000).
[34] Y. L. Klimontovich, *Statistical Theory of Open Systems* (Kluwer, Dordrecht, 1995).
[35] U. Erdmann, W. Ebeling, L. Schimansky-Geier, and F. Schweitzer, Eur. Phys. J. B **15**, 105 (2000).
[36] K. Franke and H. Gruler, Eur. Biophys. J. **18**, 335 (1990).
[37] M. Schienbein and H. Gruler, Bull. Math. Biol. **55**, 585 (1993).
[38] A. S. Mikhailov and D. Meinköhn, in *Stochastic Dynamics*, edited by L. Schimansky-Geier and T. Pöschel, Lecture Notes in Physics Vol. 484 (Springer, Berlin, 1997), pp. 334–345.
[39] W. Ebeling and F. Schweitzer, Theor. Biosci. (to be published).
[40] W. Ebeling and F. Schweitzer, in *Integrative Systems Approaches to Natural and Social Dynamics—Systems Science 2000*, edited by M. Matthies, H. Malchow, and J. Kriz (Springer, Berlin, 2001), p. 119–142.
[41] O. Steuernagel, W. Ebeling, and V. Calenbuhr, Chaos, Solitons Fractals **4**, 1917 (1994).
[42] F. Schweitzer, *Brownian Agents and Active Particles*, Springer Series in Synergetics (Springer, Berlin, 2001).
[43] The reader is invited to view a movie of the respective computer simulations ($t=0-130$), which can be found at http://ais.gmd.de/~frank/swarm1.html
[44] The movie that shows the respective computer simulations for $t=0-100$ can be found at http://ais.gmd.de/~frank/swarm2.html